

# Lawrence Berkeley National Laboratory

## Lawrence Berkeley National Laboratory

### Title

Fermi level stabilization energy in group III-nitrides

### Permalink

<https://escholarship.org/uc/item/5fx3w23c>

### Authors

Li, S.X.

Yu, K.M.

Wu, J.

et al.

### Publication Date

2005-01-07

Peer reviewed

## Fermi level stabilization energy in group III-nitrides

S.X. Li,<sup>1,2</sup> K.M. Yu,<sup>1</sup> J. Wu,<sup>1</sup> R.E. Jones,<sup>1,2</sup> W. Walukiewicz,<sup>1</sup> J.W. Ager III,<sup>1</sup> W. Shan,<sup>1</sup> E.E. Haller,<sup>1,2</sup> Hai Lu,<sup>3</sup> and William J. Schaff<sup>3</sup>

1. Materials Sciences Division, Lawrence Berkeley National Laboratory, Berkeley, CA94720
2. Department of Materials Science and Engineering, University of California, Berkeley, CA94720
3. Department of Electrical and Computer Engineering, Cornell University, Ithaca, NY14853

### Abstract

Energetic particle irradiation is used to systematically introduce point defects into  $\text{In}_{1-x}\text{Ga}_x\text{N}$  alloys over the entire composition range. Three types of energetic particles (electrons, protons, and  $^4\text{He}^+$ ) are used to produce a displacement damage dose spanning five decades. In InN and In-rich InGaN the free electron concentration increases with increasing irradiation dose but saturates at a sufficiently high dose. The saturation is due to Fermi level pinning at the Fermi Stabilization Energy ( $E_{\text{FS}}$ ), which is located at 4.9 eV below the vacuum level. Electrochemical capacitance-voltage (ECV) measurements show that the pinning of the surface Fermi energy at  $E_{\text{FS}}$  is also responsible for the surface electron accumulation in as-grown InN and In-rich InGaN alloys. The results are in agreement with the amphoteric defect model that predicts that the same type of native defects are responsible for the Fermi level pinning in both cases.

Electronic Mail: w\_walukiewicz@lbl.gov

PACS numbers: 78.66.Fd, 61.80.-x

The discovery of the narrow bandgap of InN at  $\sim 0.7\text{eV}$  [1,2] extends the range of the direct gaps of group III-nitride alloys into the near infrared spectral region and creates the potential for new applications such as tandem solar cells [3]. An intense research effort has been aimed at elucidating the details of the electronic and optical properties of InN and In-rich group III-nitride alloys. The low value of the bandgap of InN has been confirmed by many research groups using a variety of experimental techniques [4-7]. There have been also a number of reports which argue for the bandgap values in the range from 1.2 to 1.5 eV [8,9]. It should be noted however that all InN and In-rich InGaN films are n-type as grown, with electron concentrations ranging from mid  $10^{17}$  to high  $10^{20}\text{ cm}^{-3}$ . Thus, in many instances the larger apparent values of the bandgap could be attributed to the Burstein-Moss shift of the optical absorption edge resulting from the occupation of conduction band states by free electrons [10].

The exceptional propensity of InN for n-type doping is consistent with the recent finding that the pinning of the surface Fermi level well above the conduction band edge (CBE) leads to a large surface electron accumulation [11,12]. Since the pinning energy has been found to be independent of the surface preparation conditions, native donor defects are the most likely source of the surface electrons. The above results indicate that native defects play a crucial role in determining the electronic properties of InN and In-rich group III-nitride alloys.

In this paper we report on investigation of the effects of intentionally introduced defects by high energy particle irradiation on the electronic properties of InN and  $\text{In}_{1-x}\text{Ga}_x\text{N}$  alloys. We show that the incorporation of native point defects in the bulk or on the surface is controlled by the location of the Fermi energy relative to a common energy

reference – the Fermi level stabilization energy ( $E_{FS}$ ) [13,14]. Based on our results, the extreme propensity of InN and In-rich InGaN alloys for n-type doping can be explained by the relative position of  $E_{FS}$  to the band edges.

Epitaxial InN and  $In_{1-x}Ga_xN$  thin films (310-2700 nm thick) used in this study were grown on c-sapphire substrates by molecular beam epitaxy (MBE) with a GaN (~200 nm thick) buffer layer [15]. The initial free electron concentrations in these samples as measured by Hall Effect ranged from the low  $10^{18} \text{ cm}^{-3}$  to low  $10^{17} \text{ cm}^{-3}$  and the mobility ranged from  $7 \text{ cm}^2/V\cdot\text{s}$  ( $x = 0.76$ ) to above  $1500 \text{ cm}^2/V\cdot\text{s}$  ( $x = 0$ ). A MOCVD-grown GaN sample (3  $\mu\text{m}$  thick) with electron concentration of  $7.74 \times 10^{17} \text{ cm}^{-3}$  and mobility of  $189 \text{ cm}^2/V\cdot\text{s}$  was used. An n-type GaAs samples (10-13 $\mu\text{m}$  thick,  $n_e \sim 8 \times 10^{16} \text{ cm}^{-3}$ ) was also included in this study.

The samples were irradiated with 1 MeV electrons, 2 MeV protons, and 2 MeV  $^4\text{He}^+$  particles. The fluences of electrons ranged from  $5 \times 10^{15}$  to  $1 \times 10^{17} \text{ cm}^{-2}$  and those of protons and  $^4\text{He}^+$  particles were between  $1.12 \times 10^{14}$  and  $2.68 \times 10^{16} \text{ cm}^{-2}$ . In all cases, the particle penetration depth greatly exceeded the film thickness, assuring a homogeneous damage distribution. Ion channeling spectroscopy showed that the minimum yield  $\chi$  increased from 0.04 in an as-grown InN sample to merely 0.11 after  $^4\text{He}^+$  irradiation with a dose of  $1.8 \times 10^{16} \text{ cm}^{-2}$ , indicating that the InN film remains single crystalline in spite of the high concentration of radiation-induced defects. X-ray diffraction analysis revealed that after  $^4\text{He}^+$  irradiation with a dose of  $2.68 \times 10^{16} \text{ cm}^{-2}$  the lattice parameter of the film increased by  $0.02 \text{ \AA}$  (0.35%), suggesting that point defects rather than extended defects are responsible for the observed changes in electrical and optical properties of the irradiated materials.

We used the displacement damage dose methodology developed by the Naval Research Laboratory for modeling solar cell degradation in space environments to scale the irradiation damage [16,17]. The displacement damage dose ( $D_d$ , in units of MeV/g) is defined as the product of the non-ionizing energy loss (NIEL) and the particle fluence. For the films irradiated here, the NIEL was either obtained from the tables in Ref. 16 (for electron irradiation) or from the SRIM (the Stopping and Range of Ion in Matters) program [18] (for proton and  $^4\text{He}^+$  irradiation as detailed in Ref. 17).

To avoid problems with sample inhomogeneity and variations in the properties of the metal contact in the Hall measurements, the evaluation of the proton and  $^4\text{He}^+$  particle-irradiated samples were done sequentially at progressively higher radiation doses on the same samples. Near-surface carrier concentration profiles of InGaN were measured with the Electrochemical Capacitance-Voltage (ECV) technique with 0.2M NaOH: EDTA as the electrolyte.

Figure 1 shows the electron concentrations of the irradiated InN,  $\text{In}_{0.4}\text{Ga}_{0.6}\text{N}$ , GaAs, and GaN as functions of displacement damage dose  $D_d$ . Irradiation increases the free electron concentrations in InN and  $\text{In}_{0.4}\text{Ga}_{0.6}\text{N}$ . A larger increase is found in InN where the electron concentration rises by a factor of about 300. At  $D_d$  exceeding  $10^{16}$  MeV/g, the electron concentrations saturate at a level that depends on the alloy composition. In contrast, irradiation reduces the free electron concentrations in GaN and GaAs. At  $D_d$  higher than about  $10^{13}$  MeV/g, the electron concentration in GaN decreases rapidly. The radiation-induced reduction of the free electron concentration in GaAs, which has been a well-established observation, occurs at a lower  $D_d$  of mid- $10^{12}$  MeV/g. It is important to note that although all three nitride samples had very similar starting

electron concentrations, the irradiation had a profoundly different effect on their properties. The observed increase of electron concentration in InN and  $\text{In}_{0.4}\text{Ga}_{0.6}\text{N}$  shows that the damage creates donor-like defects. On the other hand, the reduction of the electron concentration in GaN and GaAs clearly demonstrates that acceptors are the dominant radiation-induced defects in these materials.

Our results can be readily understood, using the amphoteric defect model [13,14]. Figure 2 shows the conduction band edge (CBE) and the valence band edge (VBE) energies relative to the vacuum level in  $\text{In}_{1-x}\text{Ga}_x\text{N}$ , GaAs and  $\text{Ga}_{0.5}\text{In}_{0.5}\text{P}$ . Both GaAs and  $\text{Ga}_{0.5}\text{In}_{0.5}\text{P}$  are important materials in current state-of-the-art tandem solar cells. Also shown is the Fermi level stabilization energy,  $E_{\text{FS}}$ , which is located at 4.9 eV below the vacuum level. It is important to note that the value of the electron affinity of InN (5.8 eV) is larger than that of any other semiconductor. This unique location of the CBE explains the extreme n-type activity and the effect of defects on the properties of InN. Since  $E_{\text{FS}}$  is located high in the conduction band ( $\sim 0.9$  eV above the CBE), native donors are the dominant defects introduced by irradiation damage, and, at large doses, these defects push the Fermi energy ( $E_{\text{F}}$ ) towards  $E_{\text{FS}}$ . When the damage is sufficiently high, the electron concentration saturates at a certain value (which we call  $N_{\text{S}}$ ) as  $E_{\text{F}}$  reaches  $E_{\text{FS}}$ . At this point acceptor- and donor-like defects are incorporated at the same rate and compensate each other. The Fermi level is pinned at  $E_{\text{FS}}$  and it does not change with further radiation damage. For  $\text{In}_{1-x}\text{Ga}_x\text{N}$  alloys, as  $x$  increases (more Ga), the CBE moves closer to  $E_{\text{FS}}$ , which results in a lower value of  $N_{\text{S}}$ . In  $\text{In}_{1-x}\text{Ga}_x\text{N}$  with a Ga fraction higher than 66%,  $E_{\text{FS}}$  falls below the CBE, i.e., inside the bandgap. In pure GaN,  $E_{\text{FS}}$  is located  $\sim 0.7$  eV below the CBE; therefore, in an n-type sample  $E_{\text{F}}$  lies above  $E_{\text{FS}}$  and radiation-

induced native defects are of acceptor-like character and are expected to compensate the donors, reducing the electron concentration. This is indeed what is observed in Fig. 1 for GaN. The same effect is expected (and observed) in n-type GaAs; in this case irradiation moves  $E_F$  into the lower half of the band gap, resulting in highly resistive material.

To quantify the effect of the particle irradiation on the electron concentration, we calculated  $N_S$  using the following expression [19] for a nonparabolic conduction band with  $E_F = E_{FS}$ :

$$N_S = \frac{1}{3\pi^2} \left( \frac{2m^*}{\hbar^2} \right)^{3/2} \int_{E_{CBE}}^{\infty} \frac{e^{\frac{E-E_{FS}}{k_B T}} \left[ E - E_C + (E - E_C)^2 / E_g \right]^{3/2}}{\left[ 1 + e^{\frac{E-E_{FS}}{k_B T}} \right]^2} dE, \quad (1)$$

where  $m^*$  is the band edge effective electron mass,  $E_C$  is the energy of the CBE, and  $E_g$  is the bandgap. An additional important factor is the band-gap renormalization effect [20]. At sufficiently high electron concentrations electron-electron and electron-ion interactions can significantly reduce the fundamental bandgap. Here both effects contribute to the shift of the CBE whereas the energy of the defect level is affected only by the electron-ion interaction. Consequently the net shift of the CBE with respect to the localized defect level is given only by the electron-electron interaction.

$N_S$  values of InN and  $\text{In}_{0.4}\text{Ga}_{0.6}\text{N}$  calculated from Equation (1) are marked as dotted lines in Fig. 1. They are in good agreement with the observed saturated electron concentration. Calculated values of  $N_S$  are plotted as a function of alloy composition in Fig. 3. In the calculation,  $m^*$  is extrapolated linearly between InN and GaN and a bowing parameter of 1.43 eV is used to calculate the bandgap. The calculations are in excellent agreement with experimental  $N_S$  values obtained from a number of  $\text{In}_{1-x}\text{Ga}_x\text{N}$  samples ( $0 < x < 0.76$ ) after heavy irradiation ( $D_d > 10^{16}$  MeV/g).

Our results show that, as predicted by the amphoteric defect model, incorporation of a high concentration of point defects stabilizes the Fermi energy at  $E_{FS}$ . It has been demonstrated before that the same effect is responsible for the pinning of the Fermi energy on the semiconductor surfaces [13,14]. To test this assertion we carried out measurements of the surface accumulation effect in InGaN alloys using the ECV technique. In this method a potential is applied across the electrolyte/semiconductor interface to probe the charge distribution below the semiconductor surface. A Helmholtz double layer, formed in the electrolyte, acts as an insulator whose capacitance can be changed by varying the applied bias [21]. Charge density can be obtained from the capacitance and applied bias [22]. The electron concentration profiles of a number of  $In_{1-x}Ga_xN$  alloys and their endpoint compounds (InN and GaN) are shown in Fig. 4. For comparison the calculated  $N_S$  and bulk electron concentration measured by Hall effect are also shown. The profiles of the charge distribution in the samples with  $x \leq 0.6$  clearly show an electron accumulation layer near the surface. For these samples, the carrier concentration decreases away from the surface and reaches its bulk value at the depth of few nm below the surface. The profiles also indicate that the surface accumulation effect weakens as the Ga fraction increases. As seen in Fig. 4, no surface accumulation is observed in GaN; a flat charge profile is seen with a concentration approximately equal to the bulk electron concentration.

The good agreement between the surface electron concentrations and the radiation damage-stabilized  $N_S$  indicates that in both cases the same, most likely vacancy-like, defects are responsible for the stabilization of the Fermi energy. This is the first experimental evidence that the amphoteric defect model, which has been successfully



used to describe defect behavior in standard III-V semiconductors, is also applicable to group III-nitride alloys. Using known band edge alignments [23] we can position  $E_{\text{FS}}$  in all group III-nitrides. For instance, in  $\text{In}_{1-y}\text{Al}_y\text{N}$  alloys  $E_{\text{FS}}$  falls below CBE for  $y > 0.29$ , whereas at the AlN end point it is located 2.7 eV below CBE.

In conclusion, we have shown that the incorporation of high concentration of native defects produced by high energy particle irradiation stabilizes the bulk Fermi energy in  $\text{In}_{1-x}\text{Ga}_x\text{N}$  alloys. The stabilized energy is the same as the surface Fermi level pinning energy in In-rich  $\text{In}_{1-x}\text{Ga}_x\text{N}$ . Its position ranges from 0.9 eV above the CBE in InN to about 0.7 eV below the conduction band edge in GaN. The results confirm the applicability of the amphoteric defect model to the group III-nitride alloys.

We thank W. Kemp of the Air Force Research Laboratory, Kirtland Air Force Base for performing the electron irradiation and D. Senft for helpful discussions. We also thank L. Reichertz and B. Cardozo for providing the GaAs sample and Mr. Milton Yeh of Blue Photonics Inc. for providing the GaN sample. This work is supported by the Director's Innovation Initiative Program, National Reconnaissance Office and by the Director, Office of Science, Office of Basic Energy Sciences, Division of Materials Sciences and Engineering, of the U.S. Department of Energy under Contract No. DE-AC03-76SF00098. The work at Cornell University is supported by ONR under Contract No. N000149910936.

## References:

- [1] V. Yu. Davydov, A. A. Klochikhin, R. P. Seisyan, V. V. Emtsev, S. V. Ivanov, F. Bechstedt, J. Furthmueller, H. Harima, A. V. Mudryi, J. Aderhold, O. Semchinova, and J. Graul, *Phys. Status Solidi B* **229**, R1 (2002).
- [2] J. Wu, W. Walukiewicz, K.M. Yu, J.W. Ager III, E.E. Haller, H. Lu, W.J. Schaff, Y. Saito, Y. Nanishi, *Appl. Phys. Lett.* **80**, 3967 (2002).
- [3] J. Wu, W. Walukiewicz, K. M. Yu, W. Shan, and J. W. Ager III, E. E. Haller, Hai Lu and William J. Schaff, W. K. Metzger, and Sarah Kurtz, *J. Appl. Phys.* **94**, 6477 (2003).
- [4] Y. Nanishi, Y. Saito, and T. Yamaguchi, *Jap. J. Appl. Phys.* **42**, 2549 (2003).
- [5] Fei Chen, A.N. Cartwright, Hai Lu, and William J. Schaff, *J.Cryst. Growth*, **269**, 10 (2004).
- [6] R. Goldhahn, A. T. Winzer, V. Cimalla, O. Ambacher, C. Cobet, W. Richter, N. Esser, J. Furthmüller, F. Bechstedt, Hai Lu, and W. J. Schaff, *Superlattices and Microstructures*, **36**, 591 (2004).
- [7] K. M. Yu, Z. Liliental-Weber, W. Walukiewicz, S. X. Li, R. E. Jones, W. Shan, J. W. Ager III, E. E. Haller, Hai Lu, and William J. Schaff, *Appl. Phys. Lett.* (in press).
- [8] O. Briot, B. Maleyre, S. Ruffenach, B. Gil, C. Pinquier, F. Demangeot, and J. Frandon, *J. Cryst. Growth*, **269**, 22 (2004).
- [9] T.V. Shubina, S.V. Ivanov, V. N. Jmerik, D. D. Solnyshkov, V. A. Vekshin, P. S. Kop'ev, A. Vasson, J. Leymarie, A. Kavokin, H. Amano, K. Shimono, A. Kasic, and B. Monemar, *Phys. Rev. Lett.* **92**, 117407 (2004).
- [10] J. Wu, W. Walukiewicz, S. X. Li, R. Armitage, J. C. Ho, E. R. Weber, E. E. Haller, Hai Lu, William J. Schaff, A. Barcz, and R. Jakiela, *Appl. Phys. Lett.* **84**, 2805 (2004).
- [11] I. Mahboob, T. D. Veal, C. F. McConville, Hai Lu, and W. J. Schaff, *Phys. Rev. Lett.* **92**, 36804 (2004).
- [12] V. Cimalla, G. Ecke, M. Niebelschütz, O. Ambacher, R. Goldhahn, H. Lu, and W.J. Schaff, *Phys. Stat. Sol. c* (in press).
- [13] W. Walukiewicz, *Appl. Phys. Lett.* **54**, 2094 (1989).
- [14] W. Walukiewicz, *Physica B*, **302**, 123 (2001).
- [15] H. Lu, William J. Schaff, Jeonghyun Hwang, Hong Wu, Goutam Koley, and Lester E. Eastman, *Appl. Phys. Lett.* **79**, 1489 (2001).

- [16] S. R. Messenger, G. P. Summers, E. A. Burke, R. J. Walters, and M. A. Xapsos, *Progress in Photovoltaics: Research and Applications*. **9**, 103 (2001).
- [17] S. R. Messenger, E. A. Burke, G. P. Summers, M. A. Sapsos, R. J. Walters, E. M. Jackson, and B. D. Weaver, *IEEE Trans. Nuclear Sci.* **46**, 1595 (1999).
- [18] J. F. Ziegler, J. P. Biersack, and U. Littmark, *The Stopping and Range of Ions in Solids*, vol. 1 Pergamon Press, New York (1985).
- [19] W. Zawadzki and W. Szyamańska, *Phys. Stat. Sol.* **45**, 415 (1971).
- [20] J. Wu, W. Walukiewicz, W. Shan, K. M. Yu, J. W. Ager III, E. E. Haller, Hai Lu, and William J. Schaff, *Phys. Rev. B*, **66**, 201403 (2002).
- [21] P. Blood, *Semicond. Sci. Tech.* **1**, 7-27. (1986).
- [22] William J. Schaff, Hai Lu, Lester F. Eastman, Wladek Walukiewicz, Kin Man Yu, Stacia Keller, Sarah Kurtz, Brian Keyes, and Lynn Ge, *ECS Fall 2004 Proceeding* (in press).
- [23] J. Wu, W. Walukiewicz, K.M. Yu, J.W. Ager III, S.X. Li, E.E. Haller, Hai Lu, and William J. Schaff, *Solid State Communications* **127**, 411 (2003).

Figure Captions:

Fig. 1: Electron concentrations in InN, In<sub>0.4</sub>Ga<sub>0.6</sub>N, GaN, and GaAs as a function of displacement damage dose ( $D_d$ ). Damage ranges produced by the three energetic particles: electron, proton, and  $^4\text{He}^+$  are shown. Also marked is the calculated  $N_S$  (see text) for InN and In<sub>0.4</sub>Ga<sub>0.6</sub>N.

Fig. 2: Positions of the valence band maxima and conduction band minima for InGaN alloys, GaAs, and Ga<sub>0.5</sub>In<sub>0.5</sub>P. The Fermi stabilization energy ( $E_{FS}$ ) at  $E_{vac}-4.9$  eV is also shown.

Fig. 3: The calculated  $N_S$  (solid line) and experimental saturation electron concentrations (square dots) after heavy irradiation ( $D_d > 10^{16}$  MeV/g) as function of alloy composition. A calculation performed without considering the electron-electron interaction is also shown (dotted line).

Fig. 4: ECV measurements of the electron concentration depth profile in InGaN alloys and their endpoint compounds are plotted together with their corresponding  $N_S$  values. The bulk carrier concentrations, determined from Hall Effect, are shown in the legend.

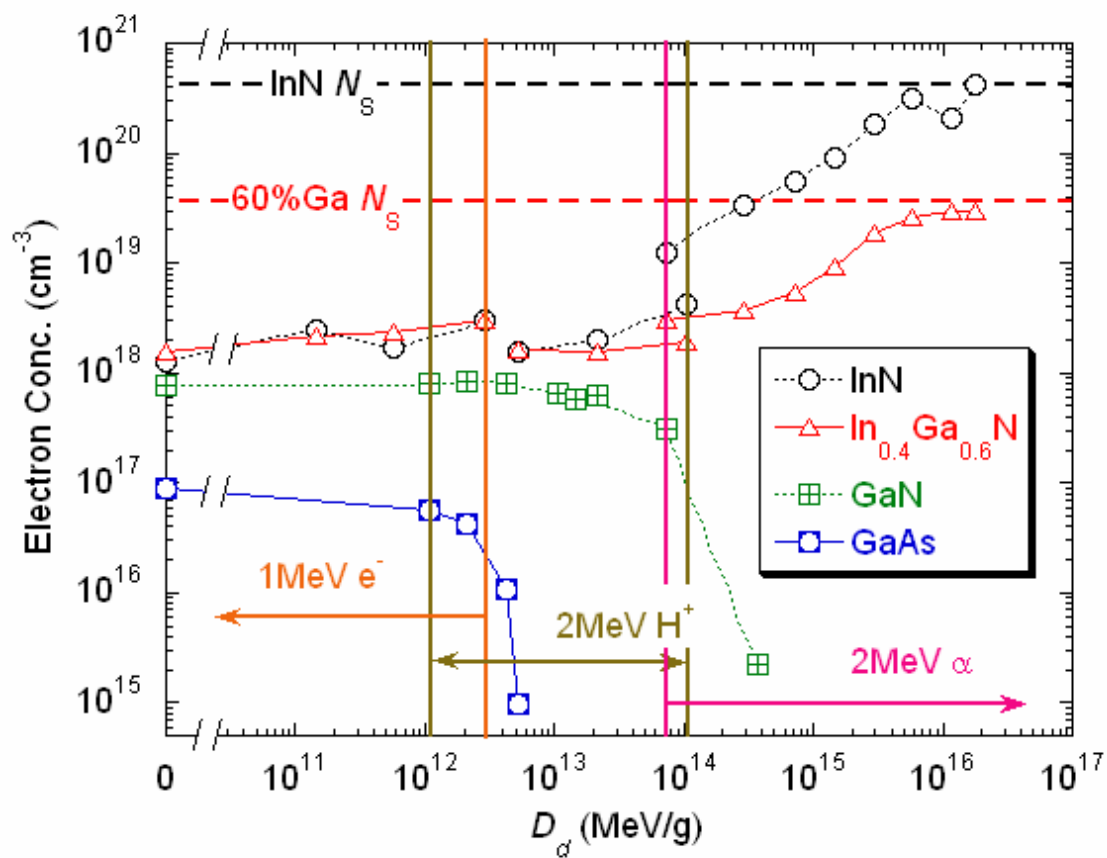


Fig. 1 of 4  
Li *et al.*

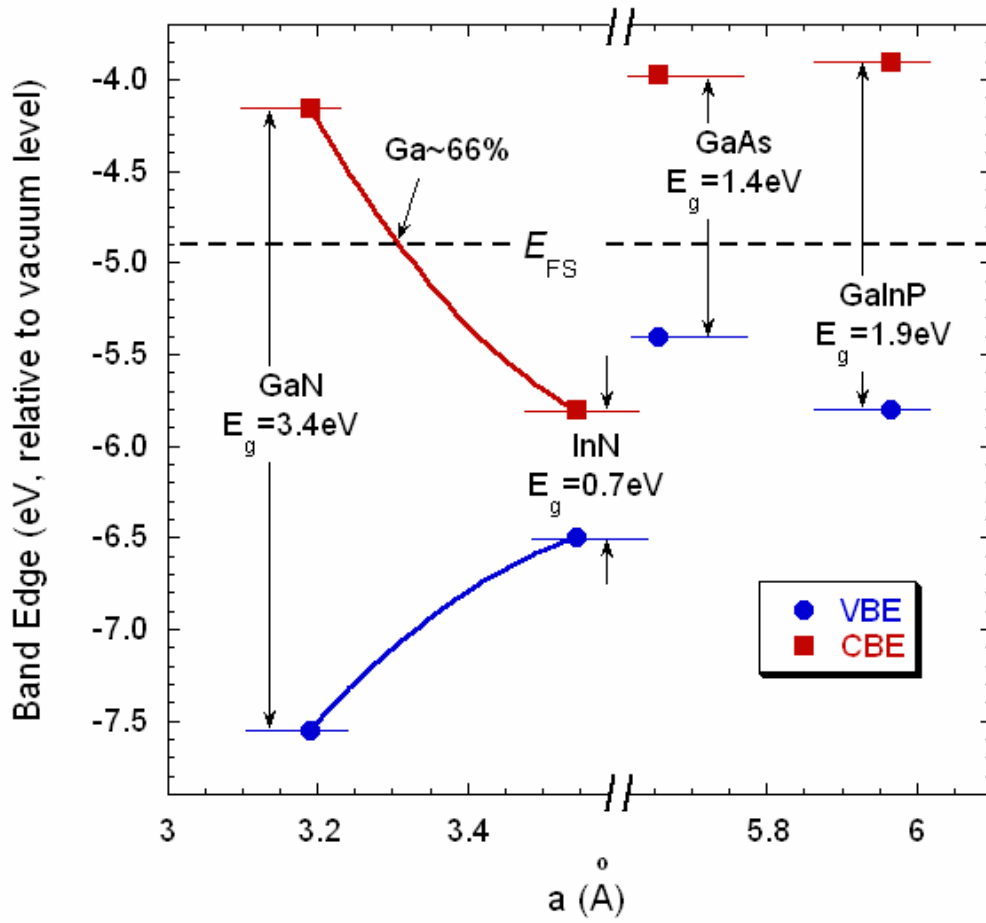


Fig 2 of 4

Li *et al.*

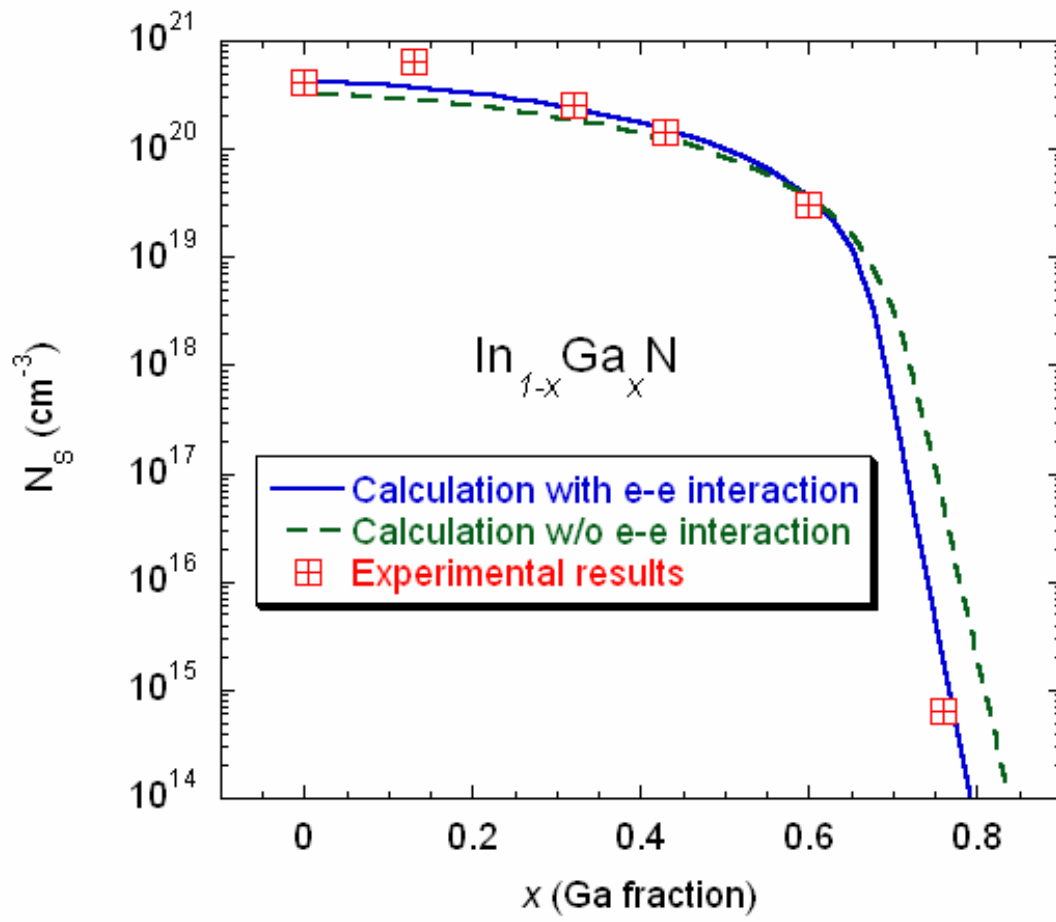


Fig. 3 of 4

Li *et al.*

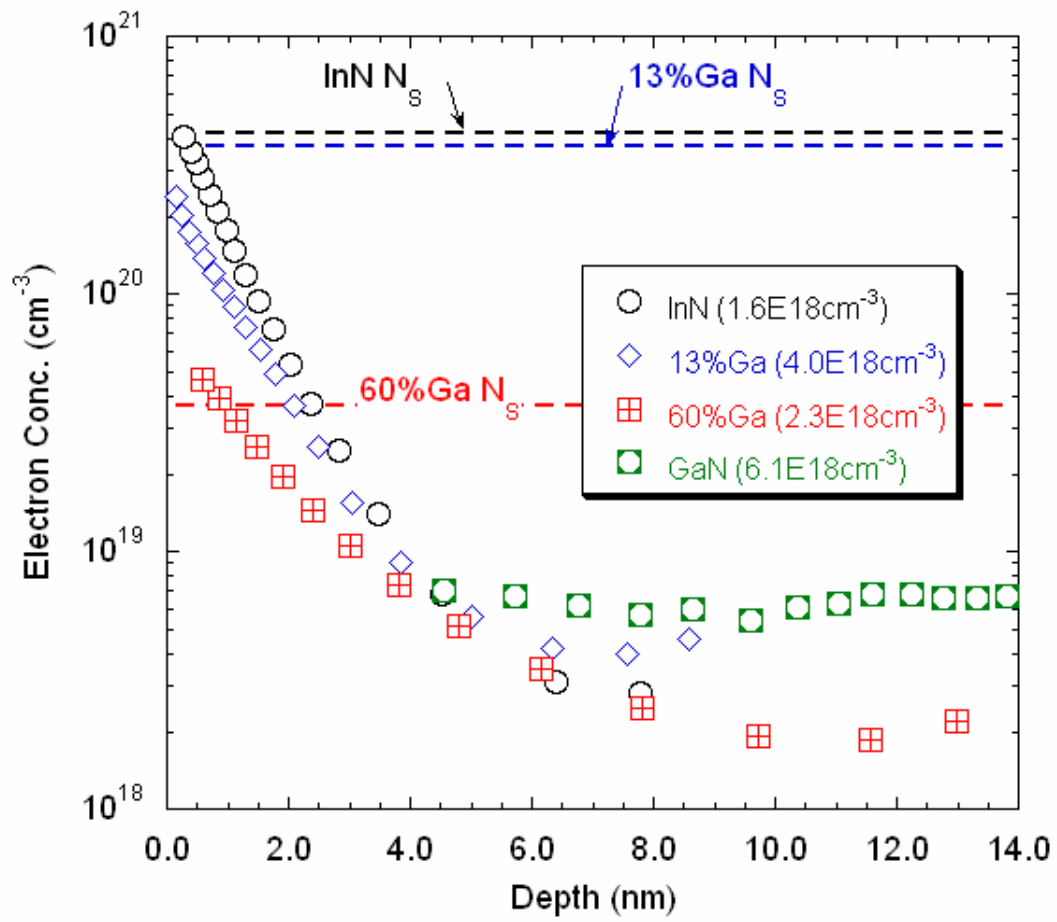


Fig. 4 of 4  
 Li *et al.*